Surface metal-insulator transition in the Hubbard model

M. Potthoff and W. Nolting
Institut für Physik, Humboldt-Universität zu Berlin, Germany

The correlation-driven metal-insulator (Mott) transition at a solid surface is studied within the Hubbard model for a semi-infinite lattice by means of the dynamical mean-field theory. The transition takes place at a unique critical strength of the interaction. Depending on the surface geometry, the interaction strength and the wave vector, we find one-electron excitations in the coherent part of the surface-projected metallic spectrum which are confined to two dimensions.

I. INTRODUCTION

The correlation-driven transition from a paramagnetic metal to a paramagnetic insulator is a fundamental problem in condensed-matter physics. The Mott transition is of interest since strong electron correlations lead to low-energy electronic properties that are qualitatively different from those predicted by band theory.

Theoretical attempts started with the early ideas of Mott [1], Hubbard [2] and Brinkman and Rice [3] (for an overview cf. [4]). In recent years a more detailed understanding has been achieved by studying the half-filled Hubbard model in the limit of high spatial dimensions d [5]. Here the electronic self-energy is a local quantity, and a self-consistent mapping onto the single-impurity Anderson model (SIAM) becomes possible [6, 7]. The impurity model can be solved numerically [7, 8, 9, 10, 11] or, for weak or strong coupling, by using perturbative approaches [6, 12]. This constitutes the dynamical mean-field theory (DMFT) which is exact for $d = \infty$ but remains a powerful method also at finite d [13, 14].

Extensive DMFT studies for the $d = \infty$ Bethe lattice with a semi-elliptic free density of states have established the following scenario for the Mott transition [14]: For strong interaction U the two high-energy charge excitation peaks are well separated by an insulating gap in the one-electron spectrum similar to the Hubbard-III approach [2]. For decreasing U the insulating solution ceases to exist at a critical value U_{c1}. On the other hand, for small U the system is a metallic Fermi liquid with a quasi-particle band at the Fermi energy. For increasing U the metallic solution of the DMFT equations coalesces with the insulating one at another critical interaction $U_{c2} > U_{c1}$. As U approaches U_{c2} the effective mass diverges as in the Brinkman-Rice solution [3]. Between U_{c1} and U_{c2} there is a region where both solutions coexist. For $T \neq 0$ the insulator is stable below U_{c2}, and the transition is of first order [14]. For $T = 0$ entropic effects favor the metallic solution. The transition is thus expected [14, 15, 16, 17] to take place at U_{c2} (second-order transition) or at least close to U_{c2}.

Although some interesting questions are yet unsolved (e. g. concerning the concept of a *pre-formed gap* for $U \mapsto U_{c2}$ [18]), one can state that there is a comparatively detailed understanding of the Mott transition in infinite dimensions. For finite dimensions one has to assume that the mean-field picture provided by the DMFT remains valid qualitatively. This is the basis for the present study which considers the Mott transition at $T = 0$, but concentrates on a new aspect of the problem: the solid surface. Surface effects are of interest for different reasons:

i) Taking into account the surface comes closer to the (inverse) photoemission experiment which determines the spectral function. The information depth in low-energy electron spectroscopy is usually limited to a few surface layers only [19].

ii) The breakdown of translational symmetry due to the surface introduces a layer dependence in the physical quantities which is worth studying. The layer dependence of the quasi-particle weight is calculated within the DMFT and also within conventional second-order perturbation theory around the Hartree-Fock solution (SOPT-HF) [20]. The perturbative treatment applies to the weak-coupling regime, non-local terms can be studied here. The (non-perturbative) DMFT accounts for the local (temporal) fluctuations exactly, but neglects all spatial correlations. Within both approaches it is found that the presence of the surface gives rise to strong oscillations depending on U and geometry.

iii) One may ask whether or not the critical interaction strength is modified at the surface, analogously to a (possibly) enhanced Curie temperature at the surface of a ferromagnet [21]. For uniform model parameters we

find a unique critical interaction U_{c2} where the whole system undergoes the transition. This excludes a surface phase different from the bulk.

iv) The low-energy electronic structure is of particular interest close to the critical point. Here but also well below U_{c2}, the surface renormalization of the one-electron excitation energies is shown to be sufficiently strong to generate a surface mode. The mode is essentially confined to two dimensions and shows up with a reduced dispersion. The generating mechanism for this type of surface excitation is exclusively due to electron correlations. A simple criterion for their existence is derived analytically.

II. MODEL AND GREEN FUNCTION

We study the Hubbard model at half-filling and $T = 0$:

$$H = \sum_{ij\sigma} t_{ij} c^\dagger_{i\sigma} c_{j\sigma} + \frac{U}{2} \sum_{i\sigma} n_{i\sigma} n_{i-\sigma} \; , \qquad (1)$$

with i and j running over the sites of a semi-infinite $d = 3$ lattice which is chosen here to be the simple cubic lattice cut at a low-index lattice plane. The uniform nearest-neighbor hopping $t_{\langle ij \rangle} \equiv -t$ with $t = 1$ fixes the energy scale. To focus on the Mott transition from a paramagnetic metal to a paramagnetic insulator, we restrict ourselves to the spin-symmetric solutions of the DMFT equations as usual [4]. Thereby, we set aside the fact that on a bipartite lattice the half-filled Hubbard model is actually in an antiferromagnetic phase below a finite Néel temperature.

We concentrate on the metallic spectrum in the vicinity of the Fermi energy. This is governed by the low-energy expansion of the self-energy [22]:

$$\Sigma_{ij}(E) = \delta_{ij} \frac{U}{2} + \beta_{ij} E + i \gamma_{ij} E^2 + \cdots \; . \qquad (2)$$

With the help of the (symmetric) matrices $\boldsymbol{\beta} = (\beta_{ij})$ and $\mathbf{Z} = (\mathbf{1} - \boldsymbol{\beta})^{-1}$ the one-electron Green function $G_{ij}(E) = \langle\langle c_{i\sigma}; c^\dagger_{j\sigma} \rangle\rangle$ can be written in the form:

$$\mathbf{G}(E) = \mathbf{Z}^{\frac{1}{2}} \frac{\mathbf{1}}{E\mathbf{1} - \mathbf{Z}^{\frac{1}{2}} \mathbf{T} \mathbf{Z}^{\frac{1}{2}}} \mathbf{Z}^{\frac{1}{2}} \; , \qquad (3)$$

where $\mathbf{G} = (G_{ij})$ and $\mathbf{T} = (t_{ij})$. Only the term linear in E is taken into account. In particular, we consider an energy range where damping effects ($\propto i\gamma_{ij} E^2$) are unimportant.

This *coherent* part of the spectrum is exclusively determined by the so-called quasi-particle weight matrix $\mathbf{Z} = (z_{ij})$ (mass-enhancement matrix $\mathbf{Z}^{-1}$). The usual *bulk* quasi-particle weight $z(\mathbf{q})$ is obtained from z_{ij} by three-dimensional Fourier transformation. For the *semi-infinite* system only lateral translational symmetry can be exploited. Considering the system to be built up by $N_\perp$ layers parallel to the surface ($N_\perp \mapsto \infty$), there is a collection of $N_\perp$ one-dimensional Fermi-"surfaces" in the two-dimensional surface Brillouin zone (SBZ). The μ-th Fermi surface is given by $\epsilon_{\mathbf{k}\mu} = 0$ where $\epsilon_{\mathbf{k}\mu}$ ($\mu = 1, ..., N_\perp$) are the eigenvalues of the renormalized hopping matrix $\mathbf{Z}^{\frac{1}{2}} \mathbf{T} \mathbf{Z}^{\frac{1}{2}}$ at a two-dimensional wave vector $\mathbf{k}$ of the SBZ. The corresponding eigenvectors $\mathbf{u}_{\mathbf{k}\mu}$ yield the discontinuous drops of the momentum distribution function along the direction $\mathbf{k}$ in the SBZ via: $\delta n(\mathbf{k} = \mathbf{k}^\mu_{\rm F}) = N_\perp^{-1} \mathbf{u}^\dagger_{\mathbf{k}\mu} \cdot \mathbf{Z} \cdot \mathbf{u}_{\mathbf{k}\mu}$. For $N_\perp \mapsto \infty$ the decrease of $n(\mathbf{k})$ is continuous, the quasi-particle weight matrix $\mathbf{Z}$, however, has a well-defined meaning according to Eq. (3).

III. PERTURBATIONAL APPROACH

$\mathbf{Z}$ shall be calculated at a mean-field level assuming that spin and charge fluctuations are reasonably *local*. This implies a local self-energy, $\Sigma_{ij} \approx \delta_{ij} \Sigma_i$, which needs justification for $d < \infty$ and in particular for the $d = 3$ semi-infinite lattice. Some insight can be gained by conventional second-order perturbation theory around the Hartree-Fock solution. SOPT-HF is capable of accounting for the complete non-locality of the self-energy in the weak-coupling regime also for the case of reduced translational symmetry [20].

We have calculated the linear coefficient β_{ij} for the different low-index surfaces. The low-energy expansion of the SOPT-HF self-energy yields:

$$\beta_{ij} = -2U^2 \int_0^\infty dx \int_0^\infty dy \int_0^\infty dz \, \frac{\rho^{(0)}_{ij}(x) \rho^{(0)}_{ij}(y) \rho^{(0)}_{ij}(z)}{(x+y+z)^2} \; , \qquad (4)$$

if the HF (on- or off-site) density of states is symmetric, $\rho^{(0)}_{ij}(-E) = \rho^{(0)}_{ij}(E)$, and $\beta_{ij} = 0$ if it is antisymmetric. Fig. 1 shows the local term $\beta_{i=j}$ to exhibit a weak layer dependence for the sc(100) surface. Only for the topmost surface layer a significant difference to the bulk value is found. Surface effects become stronger for the sc(110) and are most pronounced for the sc(111) surface where a strong oscillation of β_{ii} is noticed. This can be understood as follows: According to Eq. (4) the dominant contribution to β_{ii} comes from the HF density of states density near $E = 0$. For the sc(111) surface, however, the $E = 0$ value is known [23] to oscillate be-

tween zero (for the sub-surface and all even layers) and a constant value (for the topmost and all odd layers). This anomalous behavior is found [23] to dominate the shape of the density of states within an energy range $\Delta E \sim tL^{-2}$, where L denotes the distance to the surface. Passing from the surface to the volume, $L \mapsto \infty$, the bulk HF density of states is recovered outside an infinitesimally small energy range around $E = 0$. For the coefficient β_{ii} this implies a damped layer-by-layer oscillation with the maximum absolute value for the topmost layer.

For the discussion of the non-local terms $\beta_{i\neq j}$ we have to consider second nearest-neighbors since electron-hole symmetry requires $\rho^{(0)}_{ij}(E)$ to be antisymmetric and thus $\beta_{ij} = 0$ for nearest neighbors i, j on a bipartite lattice and at half-filling. We also find surface-induced oscillations in the case $i \neq j$ as can be seen in Fig. 1. More important, however, the absolute values are smaller by

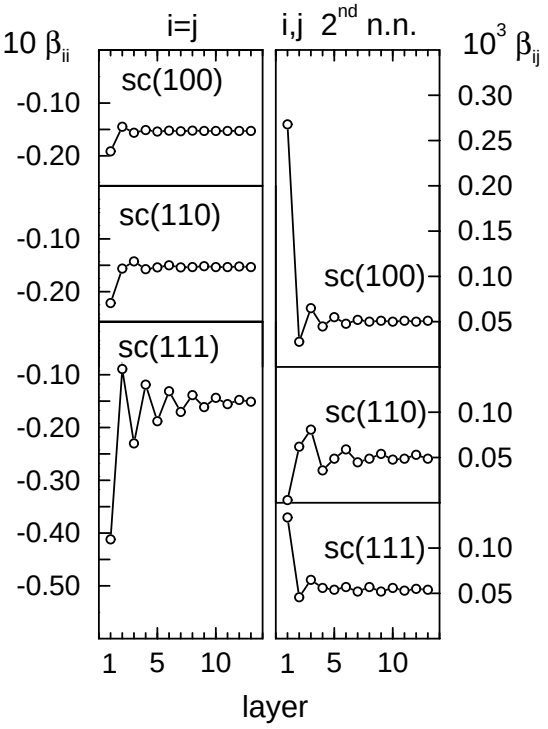

Fig. 1. Layer dependence of the on-site (left) and the off-site (right) linear coefficient in the low-energy expansion (2) of the self-energy at different surfaces of the s.c. lattice as obtained within SOPT-HF. Second-nearest neighbors i and j within the same layer. Within SOPT-HF $\beta_{ij} \sim U^2 \times$ const.; we set $U = 1$ in the figure. Note the different scales. Energy units such that $t = 1$.

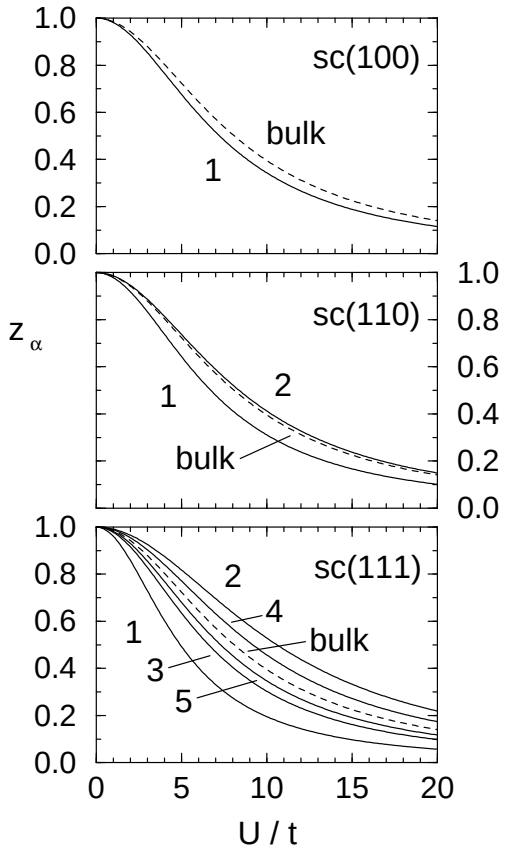

Fig. 2. U dependence of the layer-dependent quasi-particle weight $z_\alpha = (1 - \beta_\alpha)^{-1}$ within SOPT-HF. Results for different surfaces. '1' stands for the topmost surface layer. Dashed lines: bulk s.c. lattice.

about *two orders of magnitude* compared with the local terms.

Let us consider the quasi-particle weight matrix. Decomposing the linear coefficient into local and non-local parts, $\beta_{ij} = \delta_{ij}\beta_{ij} + (1 - \delta_{ij})\beta_{ij}$, and expanding $\mathbf{Z} = (\mathbf{1} - \boldsymbol{\beta})^{-1}$ in powers of the non-local one, yields

$$\Delta z_{ii} = \sum_{j}^{j\neq i} \frac{1}{1-\beta_{ii}} \beta_{ij} \frac{1}{1-\beta_{jj}} \beta_{ji} \frac{1}{1-\beta_{ii}} \qquad (5)$$

for the lowest-order non-local correction Δz_{ii} of the local element z_{ii}. The correction is of the order $(\beta_{i\neq j})^2$ and can thus be neglected in the weak-coupling limit.

Fig. 2 shows the local elements of the quasi-particle weight matrix $z_{ii} \approx 1/(1 - \beta_{ii})$ within SOPT-HF as a function of U. For weak coupling we observe the quadratic dependence on the interaction strength: $1 - z_\alpha(U) \propto U^2$. Depending on geometry, there is a

considerable layer dependence even for weak interaction. For strong U, SOPT-HF still predicts a Fermi-liquid state with $z_\alpha > 0$. Here, as expected, the perturbational approach breaks down.

IV. DYNAMICAL MEAN-FIELD THEORY

We now turn to the dynamical mean-field theory to consider the intermediate- and strong-coupling regime. DMFT is a non-perturbative method. However, we have to *assume* that a local self-energy functional is a reasonable approximation for $d = 3$ dimensions. From the perturbational results, this is well justified in the weak-coupling regime, for larger U the assumption may be questioned. In any case, we expect DMFT to be a good starting point.

We have generalized the mean-field equations to the case of film geometries. A film consisting of a sufficiently large but finite number of layers $N_\perp$ is considered to simulate the actual surface. Apart from mirror symmetry at the film center, the layers are treated as being inequivalent. DMFT must thus be applied in the following way: We start with a guess for the (local) self-energy $\Sigma_\alpha(E)$ for each layer (translational symmetry is assumed *within* the layers). Second, the Dyson equation is solved on the semi-infinite lattice to get the on-site Green functions $G_\alpha(E)$. For this purpose we make use of lateral translational symmetry which restricts the numerical calculations to inversion of $N_\perp \times N_\perp$ matrices on a wave-vector mesh in the two-dimensional SBZ. Corresponding to each layer α, an effective impurity problem is set up. From the on-site Green function and the self-energy, the α-th SIAM is specified by fixing the respective free impurity Green function $G^{(0)}_{\rm imp}(E)$ via the DMFT self-consistency condition:

$$G^{(0)}_{\rm imp}(E) = \left(G_\alpha(E)^{-1} + \Sigma_\alpha(E)\right)^{-1} . \qquad (6)$$

The crucial step is the solution of the (α-th) SIAM to get the self-energy $\Sigma_\alpha(E)$ which is required for the next cycle. Applying DMFT to a film geometry implies a self-consistent treatment of $N_\perp$ impurity problems that are coupled indirectly via the respective baths of conduction electrons.

For finite temperatures the impurity problems can be solved by employing the Quantum-Monte-Carlo method [7, 8, 9] using the Hirsch-Fye algorithm. For $T = 0$ the Exact-Diagonalization (ED) approach of Caffarel and Krauth [10, 11] may be applied and will be chosen for the present study. ED is able to yield the essentially exact solution of the mean-field equations in a parameter range where the errors introduced by the finite system size are unimportant. For the Mott problem the relevant low-energy scale is set by the width of the quasi-particle peak in the metallic solution. It has to be expected that there are non-negligible finite-size effects when this energy scale becomes comparatively small. We are thus limited to interactions strengths that are not too close to U_{c2} and cannot access the very critical regime.

The algorithm proceeds as follows: The DMFT self-consistency condition yields a bath Green function $G^{(0)}_{\rm imp}(iE_n)$. The parameters of a SIAM with n_s sites, the conduction-band energies ϵ_k and the hybridization strengths V_k ($k = 2, ..., n_s$), are obtained by minimizing the following cost function:

$$\chi^2 = \frac{1}{n_{\rm max}+1} \sum_{n=0}^{n_{\rm max}} \left| G^{(0)}_{\rm imp}(iE_n)^{-1} - G^{(0)}_{\rm n_s}(iE_n)^{-1} \right| , \qquad (7)$$

where $G^{(0)}_{\rm n_s}(iE_n - \mu) = (iE_n - \epsilon_d - \sum_k V_k^2/(iE_n - \epsilon_k))^{-1}$ is the free ($U = 0$) Green function of the n_s-site SIAM. The fit of $G^{(0)}_{\rm imp}(iE_n)^{-1}$ is performed on the imaginary axis, $iE_n = i(2n+1)\pi/\widetilde{\beta}$ with a *fictitious* inverse temperature $\widetilde{\beta}$ which introduces a low-energy cutoff. Lanczò's technique [24] is used to calculate the zero-temperature impurity Green function $G_{\rm imp}(iE_n)$. The local self-energy of the α-th layer is then obtained via $\Sigma_\alpha(iE_n) = G^{(0)}_{\rm imp}(iE_n)^{-1} - G_{\rm imp}(iE_n)^{-1}$. At half-filling electron-hole symmetry can be enforced by $\epsilon_k = -\epsilon_{k'}$ and $V_k^2 = V_{k'}^2$ with $k + k' = n_s + 2$.

V. RESULTS AND DISCUSSION

Routinely, the calculations have been performed for $n_s = 8$ sites. For interaction strengths well below U_{c2} this has turned out to be sufficient for convergence. The results are independent of the high-energy cutoff $n_{\rm max}$. A small low-energy cutoff ($\widetilde{\beta}W \sim 10^3$) is necessary to obtain a converged value for $1 - 1/z_\alpha = (\partial/\partial(iE))\mathrm{Im}\Sigma_\alpha(iE = 0)$. Although the film geometry implies a high-dimensional parameter space ($N_\perp(n_s - 1)/2$, i. e. ≈ 100 parameters to be determined self-consistently) we always obtained a stabilized metallic or insulating solution. A moderate number of layers $N_\perp$ in the film is sufficient to simulate the semi-infinite system. We used $N_\perp = 11, 15, 21$ layers to investigate the (100), (110) and (111) surfaces, respectively. The convergence has been checked by comparing the results from calculations for different $N_\perp$.

Difficulties arise for $U \mapsto U_{c2}$. Due to the finite

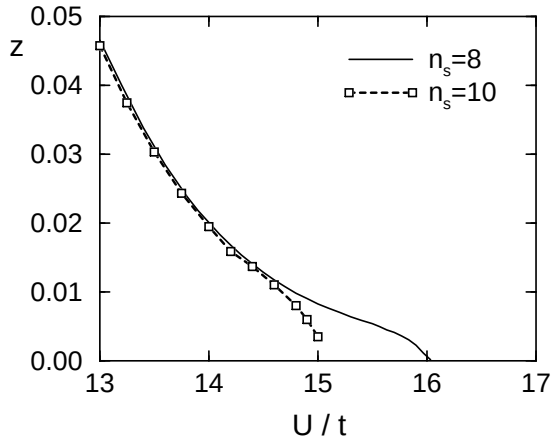

Fig. 3. Bulk quasi-particle weight as a function of U. Results for $n_s = 8$ and $n_s = 10$.

number of sites considered, the energy resolution of the conduction band cannot be better than $\Delta E \approx \eta W/n_s$, where W is the free band width and η is a constant which accounts for the fact that the conduction-band energies ϵ_k are not equally spaced and depend on U. ΔE can be estimated by comparing the results for different n_s. Fig. 3 shows the bulk quasi-particle weight z as a function of U as obtained from calculations for $n_s = 8$ and $n_s = 10$ sites. We notice that there is a good agreement between both results for U smaller than ~ 14.5 or z larger than ~ 0.01. For $z < 0.01$ the energy scale set by the width of the quasi-particle peak $\approx zW$ can no longer be resolved, i. e. $\Delta E \approx 0.12 = W/100$. For $n_s = 8$ and $U = 15$ this ΔE is also the typical energetic distance between the conduction-band level at the Fermi energy, $\epsilon_k = 0$, and the level with lowest absolute energy $\epsilon_{k'} \neq 0$ in the self-consistent solution. The error that is introduced by the low-energy cutoff $\widetilde{\beta}$ is found to be of minor importance compared with the error due to finite-size effects. This is ensured by choosing $\widetilde{\beta}$ such that $\pi\widetilde{\beta}^{-1}$ (≈ 0.03) is smaller than ΔE.

From the zero of $z(U)$ in Fig. 3 we can estimate the critical interaction: $U_{c2} \approx 16t = 1.33W$ for $n_s = 8$ and $U_{c2} \approx 15t = 1.25W$ for $n_s = 10$. Obviously, a precise determination is not possible. The results may be compared with the value $U_{c2} \approx 1.34W$ which has been obtained for the Bethe lattice with infinite connectivity using ED at a finite but low temperature $\beta t = 100$ [25]. For interaction strengths $U > U_{c1} = 11.5t$ we also obtain an insulating solution. Contrary to U_{c2}, the value found for U_{c1} is almost independent of n_s. This is plausible since there is no small energy scale in the case of the insulator.

We now return to our main subject of interest: the layer and interaction dependence of the quasi-particle weight at the surfaces of the s.c. lattice. Fig. 4 shows the results obtained for $n_s = 8$. At weak coupling we notice a quadratic U dependence consistent with perturbation theory. For the sc(100) surface there are no significant differences between the DMFT and the SOPT result for z_α up to $U \approx 2 - 3$ (see top panel in Fig. 4). The same holds for the sc(110) surface (not shown). Contrary, perturbation theory breaks down at a much weaker interaction strength for the sc(111) surface as it is obvious comparing the results in Figs. 2 and 3.

For low and intermediate U, z_α has an oscillating layer dependence while it is monotonous close to the transition (Fig. 4, insets). The strongest surface effects are seen for the open sc(111) surface while for the sc(100) surface $z_\alpha \approx z_{\rm bulk}$ except for $\alpha = 1$. This trend is related to the decrease of the surface coordination numbers: $n_{\rm S}^{(100)} = 5$, $n_{\rm S}^{(110)} = 4$, $n_{\rm S}^{(111)} = 3$, to be compared with the bulk value $n_{\rm B} = 6$.

For all surfaces and layers there is a unique and common critical interaction U_{c2} where $z_\alpha(U)$ approaches zero. The value of U_{c2} is the same as the bulk critical interaction strength (found for $n_s = 8$), i. e. U_{c2} is determined by the bulk system. In all cases the quasi-particle weight of the topmost layer $z_{\rm S}$ is significantly reduced with respect to the bulk value z. This is plausible since the variance $\Delta = n_{\rm S}t^2$ of the free ($U = 0$) surface density of states is smaller due to the reduced surface coordination number $n_{\rm S}$, and thus $U/\sqrt{\Delta}$ is larger at the surface which enhances correlation effects. The reduced surface coordination number therefore *tends* to drive the surface to an insulating phase at an interaction strength lower than the bulk critical interaction U_{c2} ($z > 0$, $z_{\rm S} = 0$). A real surface transition, however, is not found; $z_{\rm S}$ remains to be non-zero up to U_{c2}.

This is interpreted as follows: For $U < U_{c2}$ the bulk quasi-particle band has a finite dispersion. The corresponding low-energy excitations are thus extended over the entire lattice. Due to hopping processes between the very surface and the bulk, they will have a finite weight also in the top layer. Therefore, below U_{c2} the bulk excitations will to some extent *induce* a quasi-particle peak with a non-zero weight $z_{\rm S} > 0$ in the topmost layer. To test this interpretation, we decoupled the top layer from the rest system by switching off the hopping between the top and the subsurface layer, $t_{12} = 0$. For the sc(111) surface this implies $n_{\rm S} = 0$. The top-layer self-energy is thus given by the (insulating) atomic-limit expression

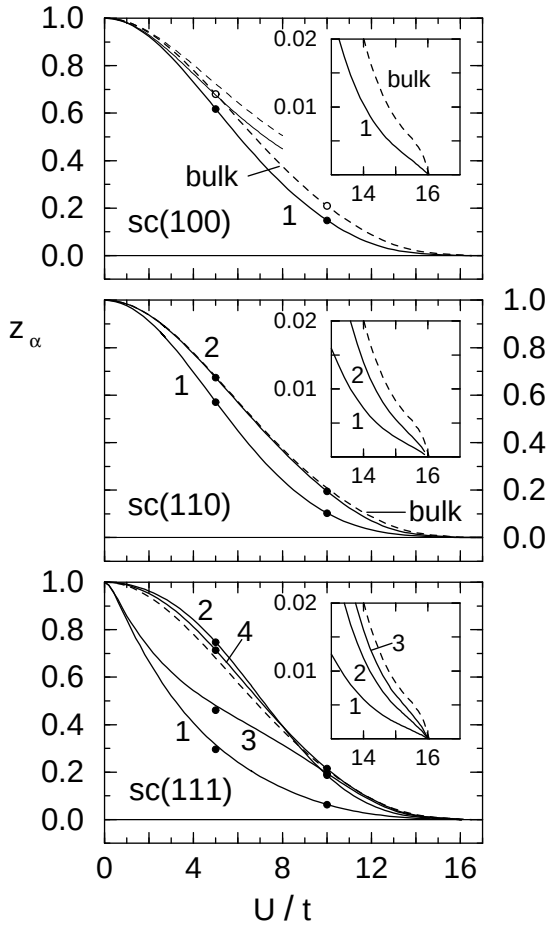

Fig. 4. U and layer dependence of $z_\alpha = (1-\beta_\alpha)^{-1}$ in the vicinity of the surface (bulk: dashed lines). ED calculation for 8 sites (filled/open circles: $n_s = 10$). $N_\perp = 11, 15, 21$ for the sc(100), sc(110), sc(111) surface, respectively. Insets: z_α in the critical regime. Thin (solid and dashed) lines: SOPT-HF results for the sc(100) surface and $U < 8$ (top panel).

$\Sigma_{\alpha=1}(E) = U/2 + U^2/4E$, while for the other layers we get the same layer-dependent (metallic) self-energy as before but shifted by one layer. Taking this as the starting point for the DMFT self-consistency cycle where $t_{12} = t$ again, we observe that a finite quasi-particle weight in the top layer $z_S > 0$ is generated immediately and that the cycle converges to the same solution as before.

There is no Mott localization at the surface of the metallic Fermi liquid. However, the tendency of the system to reduce the surface quasi-particle weight (enhance the surface effective mass) results in a partial (wave-vector-dependent) localization of quasi-particles at the surface: Let us consider the coherent part of the surface electronic structure. To make the calculations more transparent, we assume that $z_\alpha = z$ except for the top layer ($z_{\alpha=1} = z_S$). This is well justified for the sc(100) and, except for the very critical regime, also for the sc(110) surface (Fig. 4). Furthermore, we define the ratio $r^2 = z_S/z$. Two-dimensional Fourier transformation of the renormalized hopping matrix $\overline{\mathbf{T}} = \sqrt{\mathbf{Z}}\mathbf{T}\sqrt{\mathbf{Z}}$ yields a tridiagonal matrix $\overline{T}_{\alpha\alpha'}(\mathbf{k})$ in the layer indices $\alpha, \alpha' = 1, ..., N_\perp$. For $\alpha, \alpha' \geq 2$ the non-zero elements are given by $\overline{T}_{\alpha\alpha}(\mathbf{k}) = z\epsilon_\parallel(\mathbf{k})$ and $\overline{T}_{\alpha\alpha\pm1}(\mathbf{k}) = z\epsilon_\perp(\mathbf{k})$. For the sc(100) surface the parallel and perpendicular dispersions read [26]: $\epsilon_\parallel(\mathbf{k}) = 2t(\cos(k_x a) + \cos(k_y a))$ and $\epsilon_\perp(\mathbf{k}) = t$. At the very surface we have: $\overline{T}_{11}(\mathbf{k}) = r^2 z\epsilon_\parallel(\mathbf{k})$ and $\overline{T}_{12/21}(\mathbf{k}) = rz\epsilon_\perp(\mathbf{k})$. The specific surface renormalization ($r^2 < 1$) leads to two (localization) effects relevant on the energy scale zW: a diminished parallel dispersion in the top layer and a tendency to decouple the top-layer from the bulk spectrum.

As a consequence, surface excitations split off the continuum of bulk excitations in the SBZ: For tridiagonal $\overline{T}_{\alpha\alpha'}(\mathbf{k})$ the $\mathbf{k}$-resolved surface Green function is readily calculated [24]; we have:

$$G_0(\mathbf{k}, E) = z\frac{1}{2b^2}\big(E - a \mp \sqrt{(E-a)^2 - 4b^2}\big) \quad (\text{for} \quad \pm\,\mathrm{Re}(E-a) > 0)\,, \tag{8}$$

with $a \equiv z\epsilon_\parallel(\mathbf{k})$, $b \equiv z\epsilon_\perp(\mathbf{k})$ for the unperturbed surface ($r^2 = 1$). Thus, for $r^2 = 1$ the coherent part of the surface spectral density $-\mathrm{Im}G_0(\mathbf{k}, E + i0^+)/\pi$ is semi-elliptical for each $\mathbf{k}$ with band edges at $E = a \pm 2b$. The surface Green function G for the perturbed surface ($r^2 < 1$) can be expressed in terms of G_0 as [24]:

$$G(\mathbf{k}, E) = \frac{z_S}{E - r^2 a - r^2 b^2 G_0(\mathbf{k}, E)}\,. \tag{9}$$

A surface excitation is characterized by an energy that (for a given wave vector $\mathbf{k}$ of the SBZ) falls outside the continuum of bulk excitations described by G_0. A condition for the existence of surface excitations is therefore given by $|E_S - a| > 2b$ where E_S is the excitation energy obtained from the perturbed surface Green function: $G(\mathbf{k}, E = E_S)^{-1} = 0$. With $G_0(\mathbf{k}, E) = \pm z/b$ at the band edges $E = a \pm 2b$ this is equivalent to:

$$0 > 2b^2 \pm b(a - a_0) - b_0^2\,, \tag{10}$$

where $a_0 \equiv r^2 z\epsilon_\parallel(\mathbf{k}) = r^2 a$ and $b_0 \equiv rz\epsilon_\perp(\mathbf{k}) = rb$. Eq. (10) generally tells us whether or not a discrete eigen-

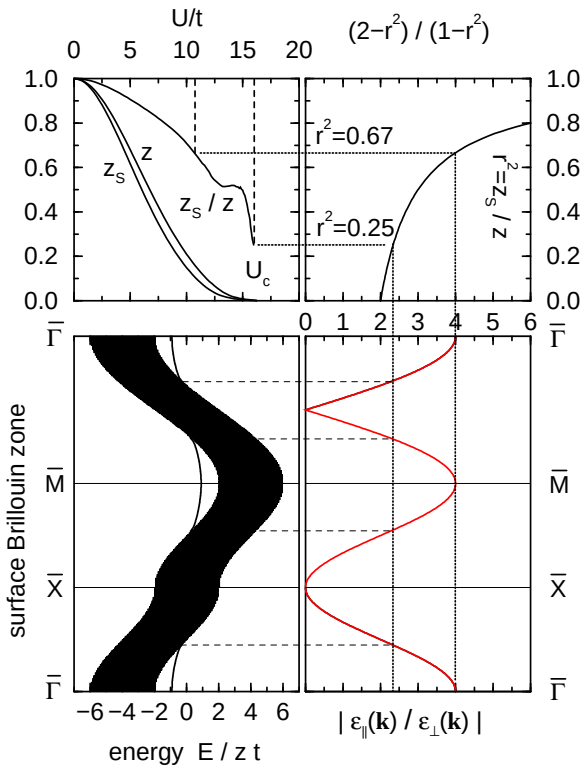

Fig. 5. *Upper left:* $z(U)$, $z_{\rm S}(U)$ and the ratio $r^2 = z_{\rm S}/z$ for the sc(100) surface. *Upper right:* $(2-r^2)/(1-r^2)$ as a function of r^2. *Lower right:* Ratio between parallel and perpendicular dispersion along high-symmetry directions in the two-dimensional surface Brillouin zone (SBZ). At $\mathbf{k}$ points with $(2-r^2)/(1-r^2) < |\epsilon_\parallel(\mathbf{k})/\epsilon_\perp(\mathbf{k})|$ surface excitations are split off the bulk continuum. *Lower left:* Coherent part of the quasi-particle spectrum projected onto the SBZ calculated from Eqs. (8) and (9). Filled area: bulk continuum. Solid line: surface excitation for $r^2 = 0.25$ corresponding to $U = U_{c2}$.

value is split off the eigenvalue continuum of a semi-infinite tridiagonal matrix with modified "surface" parameters. For the present case it immediately leads to the following simple criterion for the existence of a surface excitation:

$$\frac{2-r^2}{1-r^2} < \left|\frac{\epsilon_\parallel(\mathbf{k})}{\epsilon_\perp(\mathbf{k})}\right| . \qquad (11)$$

Hereby, the ratio $r^2 = z_{\rm S}/z$ is related to the ratio between the free dispersions.

Fig. 5 visualizes the criterion for the case of the sc(100) surface. At small U, the renormalization factor r^2 is too close to 1 to generate surface excitations. These appear above $U \approx 11t$ and split off the bulk continuum at the $\overline{\Gamma}$ and $\overline{M}$ high-symmetry points in the SBZ. The minimum interaction strength is well below U_{c2}. Finite-size effects are of no importance here. For $U \mapsto U_{c2}$ surface excitations are found in a fairly extended region around $\overline{\Gamma}$ and $\overline{M}$. In the insulating phase the whole coherent spectrum diappears. The sc(110) surface is even more favorable for surface excitations. Eq. (11) always holds along the $k_y = \pi/\sqrt{2}a$ direction where $\epsilon_\perp(\mathbf{k}) = 0$ [26]. For the sc(111) surface z_α deviates from z also in some subsurface layers. Calculating the coherent surface spectrum from the DMFT results for $z_\alpha(U)$ shows that surface excitations do not exist for any U.

As can be seen in Fig. 5, the surface excitation splits off the bulk continuum away from the Fermi energy. Due to quasi-particle damping the surface peak in the spectrum will therefore aquire a finite width which is of the order $\Delta E \approx z_{\rm S} \cdot |\gamma_{\rm S}| E_{\rm S}^2$ where $\gamma_{\rm S}$ is the damping coefficient at the surface defined in Eq. (2). Since we have $E_{\rm S} \approx z_{\rm S} t$ for the position of the excitation, the width is $\Delta E \approx z_{\rm S}^3 |\gamma_{\rm S}| t^2$. For $U \mapsto U_{c2}$ ($z \mapsto 0$) the E^2 coefficient in the expansion of the self-energy diverges as $\gamma \sim -1/z^2 W$ as has been shown in Ref. [16] for the $d = \infty$ Bethe lattice. This result may be used to estimate $\Delta E < z_{\rm S} t$. Comparing ΔE with the energetic distance between the surface peak and the edge of the bulk continuum, $|E_{\rm S} - E_{\rm B}| \approx zt$ (Fig. 5), shows both quantities to be of the same order of magnitude for $U \mapsto U_{c2}$. We conclude that the surface peak cannot be fully separated in energy from the bulk features in the surface-projected spectrum.

A complete energetic separation between bulk and surface excitations is possible if $E_{\rm S}$ crosses the Fermi energy as a function of $\mathbf{k}$. The dispersion of the surface mode can be calculated from (8) and (9) to be:

$$E_{\rm S}(\mathbf{k}) = \frac{1}{2} z r^2 \epsilon_\parallel(\mathbf{k}) \pm z r^2 \sqrt{\frac{\epsilon_\parallel(\mathbf{k})^2}{4} - \frac{\epsilon_\perp(\mathbf{k})^2}{1-r^2}} . \qquad (12)$$

Setting $E_{\rm S}(\mathbf{k}) = 0$ yields $\epsilon_\perp(\mathbf{k}) = 0$. As mentioned above, this is fulfilled e. g. along the $k_y = \pi/\sqrt{2}a$ direction for the sc(110) surface.

VI. CONCLUSION

While the investigation of the *surface* electronic structure of a metal has a long tradition, there are only few attempts to account for correlation effects beyond the Hartree-Fock approximation or the (ab initio) local-density approach (see [20, 27] and references therein). The present paper has focussed on the Hubbard model

as a standard model for correlated itinerant electrons and on the Mott transition as a genuine correlation effect. Adapting the dynamical mean-field theory for general film geometries and using the exact-diagonalization approach, we have investigated the specific surface properties of the $T = 0$ semi-infinite Hubbard model at half-filling.

At the surface electron-correlation effects are found to be significantly more pronounced compared with the bulk. The top-layer quasi-particle weight is considerably reduced for all surfaces and interaction strengths. Surface correlation effects are the stronger the larger is the reduction of the surface coordination number. For the comparatively open sc(111) surface there is a pronounced layer dependence of the quasi-particle weight z_α for weak and intermediate couplings. As U approaches the critical region, the layer dependence becomes monotonous in all cases.

The reduced surface coordination number *tends* to drive the system to a phase with an insulating surface on top of a metallic bulk. Eventually, however, the low-energy bulk excitations *induce* a finite spectral weight at the Fermi energy in the top-layer density of states. Consequently, all layer-dependent quasi-particle weights vanish at the same coupling strength U_{c2}; there is a unique transition point. This excludes a modified surface critical interaction and thus the existence of a surface phase.

On the other hand, a different localization effect has been found: There are special regions in the surface Brillouin zone, where the low-energy excitations in the top layer cannot couple to the bulk modes and are confined to two-dimensional lateral propagation. These surface excitations are of particular interest since their nature is rather different compared with the well-known Tamm- and Shockley-type surface states [28, 29]. Opposed to the latter they are caused by electron correlations exclusively. Quite generally, as long as the concept of a highly renormalized Fermi liquid applies, the specific surface renormalization of the effective mass tends to generate excitations split off the bulk continuum. This mechanism is sufficiently general to survive also at finite temperatures and non-bipartite lattices where antiferromagnetic order is expected to be suppressed. High-resolution photoemission from single-crystal samples of transition-metal oxides should be appropriate to detect the excitation by suitably tuning the Mott transition.

The present study has been restricted to surface geometries and uniform model parameters. It is an open question whether or not there is a surface phase if the hopping or the interaction strength at the very surface is modified. Possibly, a metallic surface coexisting with a Mott-insulating bulk can be found for a strongly reduced surface U. Future investigations may also concern thin-film geometries where the study of the thickness dependence of the critical interaction is of particular interest.

Acknowledgement

This work is supported by the Deutsche Forschungsgemeinschaft within the SFB 290.

References

[1] N. F. Mott, Philos. Mag. **6**, 287 (1961).

[2] J. Hubbard, Proc. R. Soc. London, Ser. A **281**, 401 (1964).

[3] W. F. Brinkman and T. M. Rice, Phys. Rev. B **2**, 4302 (1970).

[4] F. Gebhard, *The Mott Metal-Insulator Transition.* (Springer, Berlin, 1997).

[5] W. Metzner and D. Vollhardt, Phys. Rev. Lett. **62**, 324 (1989).

[6] A. Georges and G. Kotliar, Phys. Rev. B **45**, 6479 (1992).

[7] M. Jarrell, Phys. Rev. Lett. **69**, 168 (1992).

[8] M. J. Rozenberg, X. Y. Zhang, and G. Kotliar, Phys. Rev. Lett. **69**, 1236 (1992).

[9] A. Georges and W. Krauth, Phys. Rev. Lett. **69**, 1240 (1992).

[10] M. Caffarel and W. Krauth, Phys. Rev. Lett. **72**, 1545 (1994).

[11] Qimiao Si, M. J. Rozenberg, G. Kotliar, and A. E. Ruckenstein, Phys. Rev. Lett. **72**, 2761 (1994).

[12] T. Obermeier, T. Pruschke and J. Keller, Phys. Rev. B **56**, 8479 (1997).

[13] D. Vollhardt, In: *Correlated Electron Systems*, p. 57, ed. by V. J. Emery. (World Scientific, Singapore, 1993).

[14] A. Georges, G. Kotliar, W. Krauth, and M. J. Rozenberg, Rev. Mod. Phys. **68**, 13 (1996).

[15] M. Rozenberg, G. Moeller, and G. Kotliar, Mod. Phys. Lett. B **8**, 535 (1994).

[16] G. Moeller, Qimiao Si, G. Kotliar, M. Rozenberg, and D. S. Fisher, Phys. Rev. Lett. **74**, 2082 (1995).

[17] R. Bulla, A. C. Hewson, and T. Pruschke, preprint, cond-mat/9804224.

[18] S. Kehrein, preprint, cond-mat/9803149.

[19] C. J. Powell, J. Electron Spectrosc. Rel. Phen. **47**, 197 (1988).

[20] M. Potthoff and W. Nolting, Z. Phys. B **104**, 265 (1997).

[21] D. L. Mills, Phys. Rev. B **3**, 3887 (1971).

[22] J. M. Luttinger Phys. Rev. **121**, 942 (1961).

[23] D. Kalkstein and P. Soven, Surf. Sci. **26**, 85 (1971).

[24] R. Haydock, In: *Solid State Physics, Advances in Research and Applications*, Vol. 35, ed. by H. Ehrenreich, F. Seitz and D. Turnbull. (Academic, London, 1980).

[25] L. Laloux, A. Georges, and W. Krauth, Phys. Rev. B **50**, 3092 (1994).

[26] For the sc(110) surface we have: $\epsilon_{\parallel}(\mathbf{k}) = 2t\cos(k_x a)$, $\epsilon_{\perp}(\mathbf{k})^2 = 2t^2 + 2t^2\cos(\sqrt{2}k_y a)$, and for the sc(111) surface $\epsilon_{\parallel}(\mathbf{k}) = 0$, $\epsilon_{\perp}(\mathbf{k})^2 = 3t^2 + 2t^2\cos(\sqrt{2}k_y a) + 4t^2\cos(\sqrt{3/2}k_x a)\cos(\sqrt{1/2}k_y a)$.

[27] M. Potthoff and W. Nolting, J. Phys.: Condens. Matter **8**, 4937 (1996); Phys. Rev. B **55**, 2741 (1997); T. Herrmann, M. Potthoff and W. Nolting, Phys. Rev. B **58**, 831 (1998).

[28] I. Tamm, Physik. Zeits. Sowjetunion **1**, 733 (1932).

[29] W. Shockley, Phys. Rev. **56**, 317 (1939).